

***Ab initio* study of the magnetic structure of fcc Fe grown on a Cu(001) substrate**

B. Yu. Yavorsky,* P. Zahn, and I. Mertig

Martin-Luther Universität Halle-Wittenberg, Fachbereich Physik, D-06099 Halle, Germany

(Received 15 October 2003; revised manuscript received 26 March 2004; published 13 July 2004)

First-principle total energy studies of Fe films on a Cu(001) substrate are presented. The films are modeled by symmetric 6Fe/8Cu/6Fe slabs. Both collinear and noncollinear magnetic configurations are considered. The effect of the surface relaxation on the total energy of the system is discussed. It was found that the energy difference between the noncollinear configurations and the favored collinear double-layered antiferromagnetic state is reduced by contraction of the Fe sublayer but still remains positive. The possibility of stable noncollinear magnetic configurations in the system is discussed.

DOI: 10.1103/PhysRevB.70.014413

PACS number(s): 75.70.-i, 71.15.Nc

I. INTRODUCTION

Ultrathin films of fcc Fe grown epitaxially on a Cu(001) substrate remained for two decades a subject of great interest. One distinguishes the films grown at room temperature (RT grown) and at low temperature (LT grown).¹ They exhibit different structural and magnetic properties. Unusual magnetic behavior of the RT-grown films is of special interest. These films grow in a layer-by-layer mode with a flat surface. Despite the impressive progress in the study of magnetic and structural properties of these films the magnetic ground state of the system is still a subject of discussion. Recent measurements of the magneto-optical Kerr effect made by different experimental groups²⁻⁴ agree in predicting the surface ferromagnetism in the system but are contradictory concerning the interpretation of the bulk of the film as nonmagnetic,² antiferromagnetic,³ or noncollinear.⁴ This contradiction is probably connected to the complex, thickness dependent structure of the films. Films with fcc structure are obtained in the coverage regime of 5–10 monolayers.^{3,5} Dynamical analysis of the low energy electron diffraction (LEED) measurements⁵ showed a (2×1) reconstruction of the film surface, namely the oscillatory lateral shifts of adjacent atomic rows in (110) direction, and the expanded distance between the surface and subsurface atomic layers. Moreover, the in-plane lattice constant of the bulk of the film, determined by this analysis, was 2.52 Å, which is close to the lattice constant of the bulk fcc iron (extrapolated from the high-temperature phase) rather than that of the Cu substrate (2.55 Å). Information about chemical and structural disorder at the Fe/Cu interface is missing since the LEED measurements are not sensitive to the interface.

All these structural properties can affect the magnetic ground state of the films drastically. It is predicted theoretically that the magnetic structure of bulk fcc Fe is very sensitive to the atomic volume,⁶⁻⁹ and varies from ferromagnetism for an fcc lattice slightly expanded with respect to the Cu lattice,⁶ to the (double-layered) antiferromagnetism at the lattice constant of Cu, and further to the spin-spiral state at ~3% of the homogeneous contraction.⁹

It is very difficult, if not impossible, to include all the structural properties of the fcc Fe/Cu(001) films in a first-

principle study of the magnetic ground state. An idealized fcc structure with a lattice constant of bulk Cu serves always as a starting point for *ab initio* calculations. Total energy calculations made by different methods¹⁰⁻¹³ predict intralayer ferromagnetism and ferromagnetic coupling between the surface and subsurface Fe layers. It is also well established¹¹⁻¹³ that for the films with an even number of Fe layers ($n \geq 4$) the lowest energy among the collinear magnetic configurations possesses a double-layered antiferromagnetic (DAF) state. At the same time there is disagreement in determining the collinear magnetic state with the lowest energy for the films with an odd number of Fe layers. All the calculations detect for this case a group of nearly degenerated antiferromagnetic states. Probably, the differences in the model used for the system, e.g., free standing Fe films,¹⁰ semi-infinite,^{11,12} or superlattice¹³ geometry, or the differences in the methods of calculation are able to change the delicate energetic balance in favor of one of these configurations. This is also a possible reason for the quantitative disagreement between the first-principle results of the interlayer distances (surface relaxation) presented by different authors.^{10,12,13}

The coexistence of nearly degenerated antiferromagnetic states in the system indicates, as pointed out by Asada and Blügel,¹² the existence of a stable noncollinear magnetic configuration. Lorenz and Hafner¹⁴ calculated the magnetic ground state for fcc Fe_n/Cu(001) films with $1 \leq n \leq 7$ by means of the noncollinear real-space method based on a tight-binding-linear-muffin-tin-orbital (TB-LMTO) Hubbard Hamiltonian. Only collinear magnetic ground-state configurations were found for these thicknesses. By means of the same technique these authors studied the effect of the surface roughness and discussed noncollinear magnetic structure near the 4 ML/5 ML step in the fcc Fe/Cu(001) film.¹⁵ But this work is addressed mainly to the low-temperature-grown films.

An *ab initio* study of noncollinear magnetic structures in the Fe/Cu system based on novel experimental results⁴ was presented by Spišák and Hafner.¹⁶ The results of this work are of special importance for our study, and will be discussed in Sec. IV in detail.

In this work we apply *ab initio* total energy calculation in order to discuss both collinear and noncollinear magnetic

configurations in the system under the influence of tetragonal distortion.

II. METHOD

For the self-consistent calculations of the electronic structure of the fcc Fe/Cu(001) films we used the screened (tight-binding) Korringa-Kohn-Rostoker method (TB-KKR)^{17–19} in the atomic sphere approximation (ASA). We present the application of this method to noncollinear magnets. Therefore, we discuss the TB-KKR method and its modification to the noncollinear case in more detail.

Like a standard Green's function approach²⁰ this method is based on the Dyson equation

$$\hat{\mathbf{G}} = \hat{\mathbf{g}}_0 + \hat{\mathbf{g}}_0 \hat{\mathbf{V}} \hat{\mathbf{G}}, \quad (1)$$

but instead of the free electron Green's function, $\hat{\mathbf{g}}_0$, one uses the Green's function $\hat{\mathbf{g}}$ of the so called reference system,

$$\hat{\mathbf{g}} = \hat{\mathbf{g}}_0 + \hat{\mathbf{g}}_0 \hat{\mathbf{V}}_{\text{ref}} \hat{\mathbf{g}}. \quad (2)$$

In the simplest case the reference potential, $\hat{\mathbf{V}}_{\text{ref}}$, is the system of the constant repulsive muffin-tin (MT) potentials centered at the atomic positions. The Dyson equation has to be solved is now (in operator form):

$$\hat{\mathbf{G}} = \hat{\mathbf{g}} + \hat{\mathbf{g}} \Delta \hat{\mathbf{V}} \hat{\mathbf{G}}, \quad (3)$$

with $\hat{\mathbf{G}}$ the Green's function of the real system and $\Delta \hat{\mathbf{V}} = \hat{\mathbf{V}} - \hat{\mathbf{V}}_{\text{ref}}$ with the real potential $\hat{\mathbf{V}}$. With the angular momentum expansion in the cell centered coordinates the problem is transformed into a matrix equation,

$$G_{LL'}^{\mu\mu'}(\varepsilon) = g_{LL'}^{\mu\mu'}(\varepsilon) + \sum_{L''\mu''} g_{LL''}^{\mu\mu''}(\varepsilon) \Delta t_{L''}^{\mu''}(\varepsilon) G_{L''L'}^{\mu''\mu'}(\varepsilon). \quad (4)$$

L is a short-hand for the orbital and the magnetic quantum numbers (lm) and μ denotes atomic positions. The coefficients of the angular momentum expansion $G_{LL'}^{\mu\mu'}(\varepsilon)$ are known as structural Green's function matrix elements and $g_{LL'}^{\mu\mu'}(\varepsilon)$ are the screened structure constants. In contrast to the slowly decaying standard KKR structure constants based on a free electron Green's function the screened structure constants show a fast exponential decay. This makes the TB-KKR method particularly effective for the 2-D systems.¹⁹ The potential part in Eq. (4) is represented by the differences of the t -matrix elements for the real and the reference systems. The t -matrix becomes diagonal in ASA, $t_{LL'}^{\mu} = t_l^{\mu} \cdot \delta_{LL'}$.

We modified the method to noncollinear magnetic structures in a framework of the local spin-density approximation (LSDA)²¹ of the density functional theory (DFT).²² In this approach the effective potential of the system can be separated into single atomic contributions:

$$V_{\text{eff}}(\mathbf{r}) = \sum_{\mu} v_{\mu}(\mathbf{r} - \mathbf{r}_{\mu}) \Theta_{\mu}. \quad (5)$$

Θ_{μ} "cuts off" a volume (in our case an atomic sphere) around the μ th atomic position. For magnetic systems with

negligible spin-orbit interaction v_{μ} is a 2×2 matrix:

$$\hat{v}_{\mu}(\mathbf{r}) = w_{\mu}(\mathbf{r}) \hat{I} + \mathbf{b}_{\mu}(\mathbf{r}) \cdot \hat{\sigma}. \quad (6)$$

w_{μ} is a nonmagnetic (Coulomb) contribution, \mathbf{b}_{μ} is an internal magnetic field, \hat{I} is a 2×2 unit matrix, and $\hat{\sigma} = (\hat{\sigma}_x, \hat{\sigma}_y, \hat{\sigma}_z)$ is a vector-operator of the spin magnetic moment. For a collinear magnet the magnetization direction \mathbf{b}_{μ} can always be chosen to be parallel to the z axis of the global frame. All the single atomic contributions to the potential are in this case diagonal in the global frame,

$$\hat{v}_{\mu} = \begin{pmatrix} v_{\mu}^{\uparrow} & 0 \\ 0 & v_{\mu}^{\downarrow} \end{pmatrix}, \quad (7)$$

with v_{μ}^{\uparrow} and v_{μ}^{\downarrow} the potentials for the majority and minority electrons, respectively. The effective potential of the whole system [Eq. (5)] is, of course, also diagonal. Instead of a 2×2 matrix equation one has to solve two decoupled scalar equations with the effective potentials for the majority (minority) electrons $V_{\text{eff}}^{\uparrow(\downarrow)}$. By analogy with $v_{\mu}^{\uparrow(\downarrow)}$ one introduces $t_{l\mu}^{\uparrow(\downarrow)}$ and solves the matrix Eq. (4) for the majority and minority spins independently.

In the noncollinear case the magnetization direction changes from point to point. We restrict our consideration to the so called atomic moment approximation⁹ with a locally collinear magnetization inside a single ASA sphere. A local spin-quantization axis for the μ th atom is defined by the polar angles θ_{μ} , φ_{μ} , and a local internal magnetic field $\mathbf{b}_{\mu}(\mathbf{r})$ is directed along the unit vector

$$\mathbf{e}_{\mu} = (\sin \varphi_{\mu} \cos \theta_{\mu}, \sin \varphi_{\mu} \sin \theta_{\mu}, \cos \theta_{\mu}) \quad (8)$$

with respect to the global frame. The single atomic contributions \hat{v}_{μ} , as well as the t -matrix elements, are now nondiagonal in the global frame:

$$\tilde{t}_{l\mu}^{\mu}(\theta_{\mu}, \varphi_{\mu}) = \begin{pmatrix} t_{l\mu}^{\uparrow\uparrow} & t_{l\mu}^{\uparrow\downarrow} \\ t_{l\mu}^{\downarrow\uparrow} & t_{l\mu}^{\downarrow\downarrow} \end{pmatrix}. \quad (9)$$

It is convenient to keep the definitions for the majority and minority spin, and $t_{l\mu}^{\uparrow}$, $t_{l\mu}^{\downarrow}$, respectively, in a local frame. Using explicit expressions for $\hat{\sigma}_x$, $\hat{\sigma}_y$, and $\hat{\sigma}_z$, the t -matrix elements in a global frame are

$$\begin{aligned} t_{l\mu}^{\uparrow\uparrow} &= t_{l\mu}^{\uparrow}(1 + \cos \theta_{\mu}) + t_{l\mu}^{\downarrow}(1 - \cos \theta_{\mu}) \\ t_{l\mu}^{\uparrow\downarrow} &= (t_{l\mu}^{\uparrow} - t_{l\mu}^{\downarrow}) \sin \theta_{\mu} e^{-i\varphi_{\mu}} \\ t_{l\mu}^{\downarrow\uparrow} &= (t_{l\mu}^{\uparrow} - t_{l\mu}^{\downarrow}) \sin \theta_{\mu} e^{i\varphi_{\mu}} \\ t_{l\mu}^{\downarrow\downarrow} &= t_{l\mu}^{\uparrow}(1 - \cos \theta_{\mu}) + t_{l\mu}^{\downarrow}(1 + \cos \theta_{\mu}). \end{aligned} \quad (10)$$

The potential of the reference system can always be chosen to be spin independent. In this case the t matrix of the reference system is not affected by the transformation Eq. (10), and each matrix element of the screened structure constants should be substituted by a diagonal 2×2 matrix;

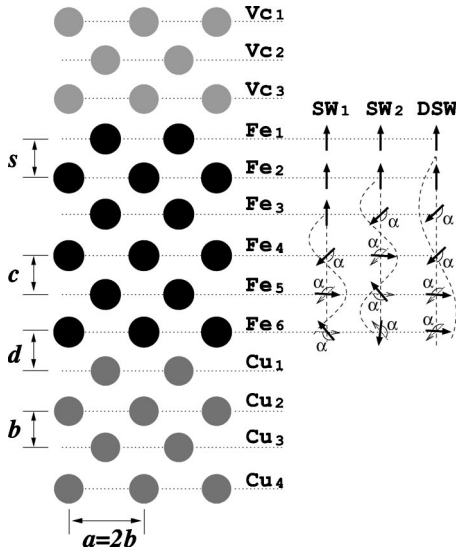


FIG. 1. Top half of the 6Fe/8Cu/6Fe slab in (001) direction of the fcc lattice (vacuum layers are also shown). The interlayer distances inside the Fe sublayer, c , between the surface and subsurface layers, s , and at the Fe/Cu interface, d , can differ from the bulk Cu value, b . Solid arrows on a right-hand part show magnetization directions for each Fe atomic layer for the three types of noncollinear magnetic structures. Dotted arrows indicate magnetization in the previous (relative to the surface) atomic layer.

$$\tilde{g}_{LL'}^{\mu\mu'} = \begin{pmatrix} g_{LL'}^{\mu\mu'} & 0 \\ 0 & g_{LL'}^{\mu\mu'} \end{pmatrix} \quad (11)$$

For systems with 3- or 2-D periodicity each atomic position \mathbf{r}_μ is a sum of a lattice vector \mathbf{R} and a position inside the unit cell \mathbf{r}_p , $\mathbf{r}_\mu = \mathbf{R} + \mathbf{r}_p$. In this case one converts the Dyson equation to the Bloch basis by means of the Fourier transformation. Finally, the modified Dyson equation becomes

$$\tilde{G}_{LL'}^{pp'}(\mathbf{k}) = \tilde{g}_{LL'}^{pp'}(\mathbf{k}) + \sum_{L''p''} \tilde{g}_{LL''}^{pp''}(\mathbf{k}) \Delta \tilde{T}_{p''}^{p''}(\theta_{p''}, \varphi_{p''}) \tilde{G}_{L''L'}^{p''p'}(\mathbf{k}). \quad (12)$$

III. CRYSTAL AND MAGNETIC STRUCTURE

We chose the following geometry for the total energy calculations. Eight layers of Cu in the (001) direction of the fcc lattice with the (cubic) lattice constant $a=3.615 \text{ \AA}$ were sandwiched on both sides by six Fe and three vacuum layers. Half of this symmetric 6Fe/8Cu/6Fe slab is shown in Fig. 1. The system was always assumed to be periodic in-plane. Interlayer distances in the Cu sublayer were kept at the bulk value $b=0.5 a$. The total energies were calculated self-consistently for several interlayer distances c in the Fe film starting from $c=b$ to $c=0.93 b$. This way we took into account (on average) a surface relaxation. In addition, at $c=0.97 b$ we considered an extra surface relaxation with increased (with respect to the bulk Cu) distances s , between the surface and subsurface Fe layers, and d , between the Fe and the Cu layers at the Fe/Cu interface, $s=d=1.05 b$. This way

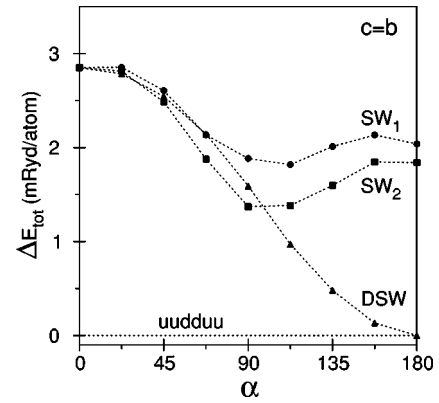


FIG. 2. Angular dependence of the total energies of the SW₁, SW₂, and DSW magnetic structures relative to the DAF state (indicated by “uudduu,” “u”, and “d” are short-hands for “spin-up” and “spin-down,” respectively) for the unrelaxed lattice.

we simulated the structural features found by various measurements.^{5,23}

We studied three types of noncollinear magnetic structures (shown in Fig. 1). In the first one three surface Fe layers (Fe₁ to Fe₃ in Fig. 1) are coupled ferromagnetically. Next, the relative angle between the magnetizations in the neighboring Fe layers (Fe₃–Fe₄, Fe₄–Fe₅, and Fe₅–Fe₆) was fixed at a constant value α . This type of the “spin-wave” magnetic structure with value $\alpha \approx 133^\circ$ extracted from the MOKE measurements was discussed by Qian *et al.*⁴ We denoted this configuration as SW₁. The next considered magnetic configuration, SW₂, is similar to SW₁, but the ferromagnetic coupling is now restricted to the surface and subsurface Fe layers only (Fe₁ and Fe₂). The “spin wave” begins now from the subsurface layer (Fe₂). This magnetic structure is of special interest because experimental and theoretical studies^{2,3,11,12} predict the ferromagnetic coupling to be restricted to the surface and subsurface Fe layers only. In the third configuration there are three pairs of ferromagnetically coupled Fe layers (Fe₁–Fe₂, Fe₃–Fe₄, and Fe₅–Fe₆). The relative angle between the magnetizations of adjacent pairs is α . By analogy with the double-layered antiferromagnetic (DAF) state we denoted this configuration as a “double-layered spin wave” (DSW). In the limiting case $\alpha=0$ all three configurations reduce to the ferromagnetic state. For $\alpha=180^\circ$ the DSW configuration presents the DAF state. The total energies were calculated self-consistently at fixed values α for $\alpha=0$ to 180° by steps of $\Delta\alpha=22.5^\circ$.

IV. RESULTS AND DISCUSSION

Angular dependencies of the total energy for the unrelaxed 6Fe/8Cu/6Fe slab ($c=b$) for the SW₁, SW₂, and DSW noncollinear magnetic configurations are shown in Fig. 2. The energy differences are presented per Fe atom relative to the DAF state. For all three dependencies the ferromagnetic state ($\alpha=0$) has always higher energy than the antiferromagnetic one ($\alpha=180^\circ$). Both the SW₁ and SW₂ configurations have a minimum at $\alpha \approx 100^\circ$, but for the SW₂ the energy in the minimum is about 0.5 mRyd lower. The DSW magnetic

structure shows a monotonic cosine-like angular dependence. The DAF state possesses the lowest energy among all the calculated magnetic configurations. This is in agreement with the previous collinear first-principle studies made for this system.^{11–13}

The angular dependence for both the SW₁ and the SW₂ magnetic configurations reproduces qualitatively the first-principle calculations of the total energy as a function of the spiral vector \mathbf{q} in the (001) direction in bulk fcc Fe with the lattice constant of Cu.^{6–9} In particular, the position of the minimum and the tendency to the antiferromagnetism, $E_{\text{tot}}(180^\circ) - E_{\text{tot}}(0) < 0$, are confirmed. At the same time our results contradict the TB-LMTO calculation presented by Spišák and Hafner who studied the same noncollinear magnetic structures in the fcc-Fe/Cu system.¹⁶ They found that the angular dependence of the total energy of the SW₁ has a pronounced maximum, and for the SW₂ shows a smooth increase. Moreover, the energy differences for the limiting cases, $\alpha=0$ and $\alpha=180^\circ$, obtained in our work opposite to the results of these authors. Let us use short-hands “u” and “d” for “spin-up” and “spin-down,” respectively. In this notation the magnetic configuration of the SW₁ for $\alpha=180^\circ$ is uudud and for the SW₂ uududu, and uuuuuu for $\alpha=0$ in both cases. We found that $E_{\text{tot}}(\text{uuuuuu}) > E_{\text{tot}}(\text{uududu}) > E_{\text{tot}}(\text{uududu})$ contrary to the result of Spišák and Hafner, who found that $E_{\text{tot}}(\text{uuuuuu}) < E_{\text{tot}}(\text{uududu}) < E_{\text{tot}}(\text{uududu})$. The last sequence is also qualitatively confirmed by the full-potential LAPW calculations of Asada and Blügel.¹² At the same time Asada and Blügel used the generalized gradient approximation (GGA) while in our work the total energies are calculated in the local spin-density approximation (LSDA).

The origin of the obtained differences should be related to the GGA. In order to check this point we included the generalized gradient corrections as proposed by Perdew and Wang²⁴ in the total energy calculations for these three collinear magnetic configurations and also the double-layered antiferromagnetic state uudduu. The interlayer distances of the Fe film were fixed, so a small strain cannot be excluded. We found the following GGA-corrected total energy differences per Fe atom:

$$E_{\text{tot}}(\text{uududu}) - E_{\text{tot}}(\text{uuuuuu}) = 1.27 \text{ mRyd},$$

$$E_{\text{tot}}(\text{uududu}) - E_{\text{tot}}(\text{uuuuuu}) = 1.48 \text{ mRyd},$$

$$E_{\text{tot}}(\text{uuuuuu}) - E_{\text{tot}}(\text{uudduu}) = 1.41 \text{ mRyd}.$$

These results agree very well, both qualitatively and quantitatively, with the calculations of Asada and Blügel.¹² The calculations of Spišák and Hafner¹⁶ were also performed within the GGA.²⁵ This is the most probable reason for the differences in the angular dependence of the total energy. Although the GGA corrections do not change the dependence on the spiral vector qualitatively in bulk fcc Fe,^{8,9} the situation may be different in layered systems.

Now we discuss the effect of the structural relaxation in the Fe sublayer on the total energy of the system. Our calculations showed that the monotonic cosine-like angular depen-

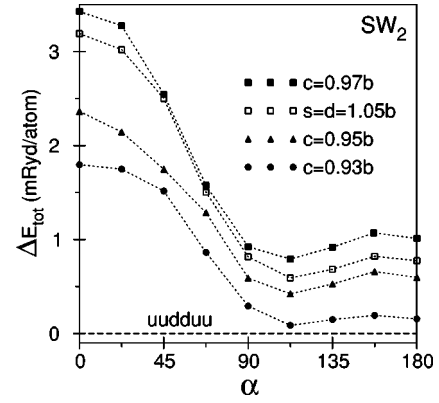


FIG. 3. Angular dependence of the total energy of the SW₂ magnetic configuration relative to the DAF state for the relaxed interlayer distances in the Fe sublayer at $c/b=0.97$, 0.95 , and 0.93 . For $c/b=0.97$ an extra 5% expansion between the surface and subsurface layers and at the Fe/Cu interface is also considered.

dence of the total energy for the DSW magnetic configuration is kept for relaxed interlayer distances up to 7% of the tetragonal contraction. Furthermore, the SW₂ magnetic structure shows for any α lower energies than the SW₁. Therefore, we focus on the energy differences between the SW₂ and the DAF states. Figure 3 shows the angular dependence of the total energy of the SW₂ relative to the DAF state for $c/b=0.97$, 0.95 , and 0.93 . It is clear that the tetragonal contraction decreases the total energy of the SW₂ state. The position of the minimum, $\alpha_{\text{min}} \approx 100^\circ$, is nearly unchanged. The difference between the minimal energy for the SW₂ and the DAF is about 0.8 mRyd for 3% and 0.4 mRyd for 5% contraction in the Fe sublayer, respectively, in comparison to about 1.35 mRyd for the unrelaxed film. It is also interesting that with the increased distances between the surface and subsurface Fe layers, s , and the interlayer distance at the Fe/Cu interface, d , by 5% ($s=d=1.05b$) for $c/b=0.97$ the energy difference is about 0.2 mRyd less than the difference for the film with 3% of the homogeneous contraction. At $c/b=0.93$ the SW₂ state with $\alpha=\alpha_{\text{min}}$ is practically degenerated with the DAF. The value 7% for the tetragonal distortion is, of course, unrealistic. Our test calculations made for bulk fcc Fe with the lattice constant of Cu showed that a tetragonal contraction of 3% already leads to a degeneration of the DAF and the spin-spiral magnetic states. This is probably the insufficient thickness of the Fe sublayer, only 6 ML, which hinders the stabilization of the fcc-Fe-bulk-like state in the layered system. On the other hand the energy difference between the collinear DAF and the noncollinear SW₂ magnetic configurations is only about 1 mRyd (per Fe atom) and decreases for the realistic interlayer distances, $c=0.97b$, $s=d=1.05b$, to about 0.6 mRyd. Small excitations due to, e.g., finite temperature can drive the system into the metastable noncollinear magnetic state. Moreover, some unknown structural properties, like a mixed Fe/Cu interface, can change the magnetic ground state of the system. Finally, we have to mention again that the variety of the possible noncollinear structures is huge. Following former calculations and new experimental results we have compared the total energy for three special types of structures to discuss general

trends in the system. But it is not a full search of the global minimum in the system.

V. CONCLUSIONS

We presented *ab initio* total energy calculation for several types of noncollinear magnetic configurations in ultrathin fcc Fe films grown on a Cu substrate. The system was modeled by the symmetric 6Fe/8Cu/6Fe slab. Among the considered magnetic structures the collinear double-layered antiferromagnetic (DAF) state is energetically preferred. It was shown that the energy difference between the favored DAF

and possible noncollinear structures is reduced by tetragonal distortion in the Fe sublayer but remains positive. The energy differences, however, are so small, less than 1 mRyd per Fe atom, that the existence of a stable noncollinear magnetic state in the system cannot be excluded.

ACKNOWLEDGMENTS

The authors would like to thank László Szunyogh, Balázs Újfalussy, László Udvardi, and Daniel Spišák for very helpful discussions. This work was supported by DFG Contract No. ME 1153/5-1 and 5-2.

*Author to whom correspondence should be addressed; electronic address: yavorsky@physik.uni-halle.de

- ¹J. Giergiel, J. Shen, J. Woltersdorf, A. Kirilyuk, and J. Kirschner, Phys. Rev. B **52**, 8528 (1995).
- ²J. Thomassen, F. May, B. Feldmann, M. Wuttig, and H. Ibach, Phys. Rev. Lett. **69**, 3831 (1992).
- ³D. Li, M. Freitag, J. Pearson, Z. Q. Qiu, and S. D. Bader, Phys. Rev. Lett. **72**, 3112 (1994); Dongqi Li, M. Freitag, J. Pearson, Z. Q. Qiu, and S. D. Bader, J. Appl. Phys. **76**, 6425 (1994).
- ⁴D. Qian, X. F. Jin, J. Barthel, M. Klaua, and J. Kirschner, Phys. Rev. Lett. **87**, 227204 (2001).
- ⁵P. Bayer, S. Müller, P. Schmailzl, and K. Heinz, Phys. Rev. B **48**, 17611 (1993); S. Müller, P. Bayer, A. Kinne, P. Schmailzl, and K. Heinz, Surf. Sci. **322**, 21 (1995).
- ⁶V. L. Moruzzi, P. M. Marcus, K. Schwarz, and P. Mohn, Phys. Rev. B **34**, 1784 (1986).
- ⁷O. N. Mryasov, A. I. Lichtenstein, L. M. Sandratskii, and V. A. Gubanov, J. Phys.: Condens. Matter **3**, 7683 (1991).
- ⁸M. Körling and J. Ergon, Phys. Rev. B **54**, R8293 (1996).
- ⁹E. Sjöstedt and L. Nordström, Phys. Rev. B **49**, 014447 (2002).
- ¹⁰T. Kraft, P. M. Marcus, and M. Scheffler, Phys. Rev. B **49**, 11511 (1994).
- ¹¹L. Szunyogh, B. Újfalussy, and P. Weinberger, Phys. Rev. B **55**, 14392 (1997).
- ¹²T. Asada and S. Blügel, Phys. Rev. Lett. **79**, 507 (1997).
- ¹³E. G. Moroni, G. Kresse, and J. Hafner, J. Phys.: Condens. Matter **11**, L35 (1999).
- ¹⁴R. Lorenz and J. Hafner, Phys. Rev. B **54**, 15937 (1996).
- ¹⁵R. Lorenz and J. Hafner, Phys. Rev. B **58**, 5197 (1998).
- ¹⁶D. Spišák and J. Hafner, Phys. Rev. B **66**, 052417 (2002).
- ¹⁷R. Zeller, P. H. Dederichs, B. Újfalussy, L. Szunyogh, and P. Weinberger, Phys. Rev. B **52**, 8807 (1995).
- ¹⁸R. Zeller, Phys. Rev. B **55**, 9400 (1997).
- ¹⁹K. Wildberger, R. Zeller, and P. H. Dederichs, Phys. Rev. B **55**, 10074 (1997).
- ²⁰W. Kohn and N. Rostoker, Phys. Rev. **94**, 1111 (1954).
- ²¹U. von Barth and L. Hedin, J. Phys. C **5**, 1629 (1972).
- ²²P. Hohenberg and W. Kohn, Phys. Rev. **136**, B864 (1964); W. Kohn and L. J. Sham, *ibid.* **140**, A1133 (1965).
- ²³H. L. Meyerheim and R. Popescu (private communication).
- ²⁴J. P. Perdew, J. A. Chevary, S. H. Vosko, K. A. Jackson, M. R. Pederson, D. J. Singh, and C. Fiolhais, Phys. Rev. B **46**, 6671 (1992).
- ²⁵D. Spišák (private communication).